

# Flow and Aspect Angle Characteristics of 12-MHz and 50-MHz Coherent Echoes

A.V. Koustov<sup>1</sup>, K. Igarashi<sup>2</sup>, D. Andr <sup>1</sup>, K. Ohtaka<sup>2</sup>, N. Sato<sup>3</sup>, H. Yamagishi<sup>3</sup>, and A. Yukimatsu<sup>3</sup>

<sup>1</sup> *Institute of Space and Atmospheric Studies, University of Saskatchewan, Saskatoon, Canada*

<sup>2</sup> *Communication Research Laboratory, Tokyo, Japan*

<sup>3</sup> *National Institute of Polar Research, Tokyo, Japan*

In this study nearly simultaneous observations of auroral coherent echoes at Antarctic Syowa station at 12-MHz (SuperDARN) and 50-MHz (CRL radar) are considered to address several issues on the plasma physics of E-region irregularities. One event with large Doppler velocities of more than 600 m/s was selected. We show for this event that while 50-MHz echoes exhibit strong flow angle variation of the power, 12-MHz echoes do not. This means that the electrojet instability evolves into a more uniform flow angle distribution of density fluctuations at decameter scales as opposed to the meter scales. In spite of the expected differences in Doppler velocities of echoes due to significantly different scales of observed irregularities, data show that the velocities are very comparable, especially for observations along the magnetic L-shells (assumed electrojet direction). The aspect angle attenuation of Doppler velocity is found to be about the same at 12- and 50-MHz and consistent with earlier observations at 50-MHz. Estimates of the aspect angle effect for power are also consistent with earlier measurements. Both factors, ionospheric propagation conditions for radio waves and plasma physical effects for irregularities are considered in an attempt to explain several observed features.

## 1. Introduction

E-region plasma irregularities have been intensively studied using 50-MHz, 140-MHz and 400-MHz coherent Doppler radars [Fejer and Kelley, 1980; Sahr and Fejer, 1996]. These observations allowed to relate various characteristics of E-region irregularities with ambient ionospheric plasma parameters, such as the intensity and orientation of the ionospheric electric field and the background plasma density gradient. These advances were supportive in identifying and establishing the plasma mechanisms responsible for the excitation of electrojet irregularities. It is well accepted now that enhanced electric fields and plasma density gradients are the main sources of free energy for the onset of the Farley-Buneman (F-B) and the gradient-drift (G-D) plasma instabilities, and consequently for the formation of E-region plasma irregularities.

Deployment of the Super Dual Auroral Radar Network (SuperDARN) HF coherent radars has opened opportunities for regular studies of decameter-scale E-region irregularities in the high-latitude ionosphere [Villain *et al.*, 1990; Hanuise *et al.*, 1991; Jayachandran *et al.*, 2000]. Though observations of every individual SuperDARN radar are interesting, measurements at Antarctic Syowa station are of a special convenience due to a doubled azimuthal coverage of the Syowa East and Syowa-South radars. Moreover, in 1995-1997, in addition to the HF radars operated by the National Institute for Polar Research (Japan), another coherent Doppler radar at 50-MHz was run by the Communication Research Laboratory (Japan). Data of this joint

experiment allow a comparative study of echo power and Doppler velocity at these significantly different frequencies and correspondingly significantly different scales. The present paper is aimed at investigation of 50-MHz and 12-MHz echo characteristics and their relation to the plasma mechanisms of meter and decameter irregularities excitation.

## 2. Experimental Setup and Observations

All three radars were closely located at Syowa (69.0S, 39.6E, magnetic latitude 67). Over 3 seasons of joint operation, there were several periods of good quality data. In this study only one event, March 17, 1997, is considered, as a first attempt to explore the common data base.

Figure 1 shows an experiment setup with the field-of-views (F-O-V) of the Syowa-East and Syowa-South SuperDARN HF radars (dark zones) and the area, outlined by the fan-like lines, where measurements have been carried out by the 50-MHz CRL coherent radar. Beam-like red lines in Figure 1 correspond to the actual beam positions of the CRL radar. The numbers by some CRL radar beams denote their azimuths, counted clockwise from the direction of geomagnetic East at Syowa (geomagnetic East is  $43.7^\circ$  to the East from geographic North). In Figure 1, PACE magnetic parallels are shown by solid curves. For convenience, the 300-km slant range marks are given by a dashed line. The solid blue curve in Figure 1 represents the line of zero off-perpendicular (aspect) angle over the scan (at 110-km altitude) assuming no refraction for radio waves.

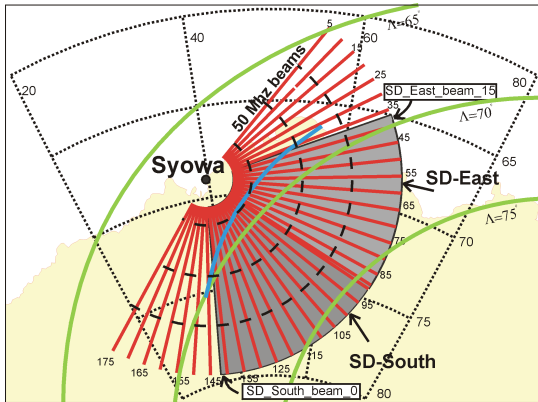


Fig 1

Both Syowa-East and Syowa-South were operating in the standard mode with scans over 16 positions. The CRL 50-MHz radar measured echo power and Doppler velocity (15-km range resolution starting from 200 km) using the double-pulse technique. Information on this radar can be found in *Igarashi et al.* [1995, 1998]. One full scan of the CRL radar was accomplished in 4 min. Strictly speaking, none of the CRL radar beam locations coincide exactly with one of the directions of the SuperDARN beams, but the differences for certain beam positions are less than  $1^{\circ}$ - $2^{\circ}$  and can be neglected, at least for the purposes of this study.

In this study we concentrate on about half an hour of data from 0100 UT to 0130 UT when westward electrojet has been established within the observational area; the Syowa station magnetometer showed a smooth negative deflection of X-component of  $\sim 150$  nT.

During 0100-0130 UT, SuperDARN echoes were mostly observed at short distances of less than 500 km with a clear maximum at distances of 250-350 km. In the CRL radar range-time intensity plot, the echoes also appeared as smooth "blobs" existing for time intervals of tens of minutes (at least several successive scans). The CRL radar showed echoes at almost all beam positions with signal-to-noise ratios of up to 40 dB in beams 35-55. The Syowa-SuperDARN radars had echoes at all directions.

Figure 2 shows the azimuthal distribution of echo power and Doppler velocity for the CRL (panels (a) and (b)) and SuperDARN (panels (c) and (d)) radars roughly over the same span of azimuths. Also plotted in Plate 1 are the curves of equal geometrical aspect angles of  $-5^{\circ}$  (for the SuperDARN panels only),  $-2^{\circ}$ ,  $0^{\circ}$ , and  $+2^{\circ}$ . One can clearly see, panels (a) and (b), that 50-MHz echoes have power and velocity maxima close to the line of zero aspect angle though there is a tendency for the power contours to be shifted slightly equatorward, towards the line of  $-1^{\circ}$  aspect angle. For these echoes, one can also clearly recognize the strong power and velocities for the azimuths of 80-100, i.e. for observations approximately along the L-shells, an assumed direction of the electron flow. Power is minimal for azimuths  $\sim 130$

(roughly perpendicular to the magnetic L-shells) so that even data gaps are seen.

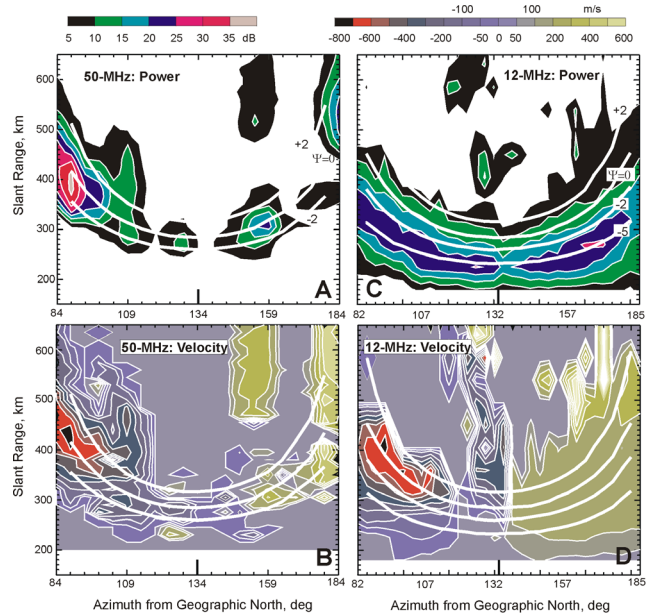


Fig. 2

Interestingly, there is a local power enhancement at azimuths 150. Velocity of 50-MHz echoes decreases with azimuth and eventually, at azimuths 140, changes its sign from negative to positive values. Stronger positive velocities have been observed at beam positions 185-195 (outside the area of SuperDARN measurements, data are not presented here) indicating that the L-shell aligned flow was extended into the earlier time sector. SuperDARN 12-MHz data, panels (c), also exhibit an "arc-like" distribution of echo power though clearly there is no drastic change of echo power with azimuth. Obviously also that echoes are much more shifted towards shorter distances and centered around the  $-5^{\circ}$  aspect angle line. Echo power has minimum for the directions roughly across L-shells, though this power decrease is not significant. Notice a local power enhancement at azimuths about 165, i.e. close to the directions where the local power enhancement was detected by the 50-MHz radar. Velocity distribution, panel (c), at a first glance, has the morphology similar to the 50-MHz echoes; negative large velocities at azimuths of 80 - 100 (along the electron flow) are gradually replaced by smaller (in absolute value) velocities at larger azimuths so that eventually the polarity of the velocity changes at the azimuth of 130 (roughly the magnetic meridian). However, there is a difference of SuperDARN velocities for poleward and westward azimuths in a sense that they do not show so strong increase for the azimuths 175 - 185 as do the 50-MHz echoes.

Another distinct feature of the SuperDARN data is the fact that, for observations at azimuths 80 - 100, the slant ranges for the power and velocity maxima are significantly different. One can

see that echo power is maximized about 50 km equatorward of the Doppler velocity maximum.

Though great similarities in echo power and velocity distributions are seen in Figure 2, a more detail scrutiny indicates some noticeable differences. To show some of these differences in a clear form, we present echo range profiles for nearly the same azimuths of 50-MHz and 12-MHz measurements. Figure 3 shows the power and Doppler velocity versus distance for both radar systems.

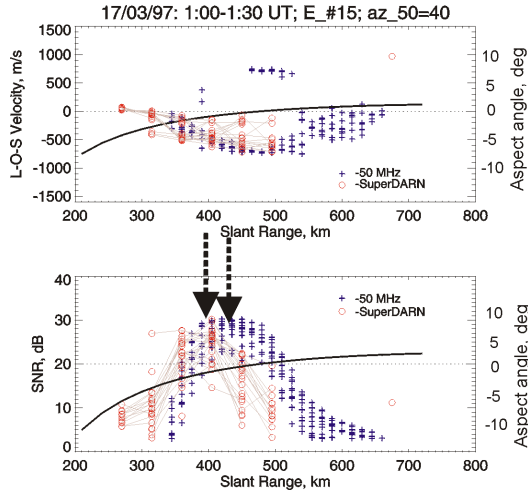


Fig. 3

We consider here beam #15 for Syowa East and beam #40 for the CRL radar. The SuperDARN and CRL data are shown by circles and crosses, respectively. Dashed curve in this diagram represents the geometrical aspect angle at various slant ranges. The scale of aspect angles is indicated on the right-hand-side of the plot. Angles are  $-15^\circ$  at short ranges of 200 km, around zero at 480 km and up to  $+2^\circ$  in the interval of ranges 500-700 km. The top panel in Figure 3 shows that the observed velocities are very close to each other at distances 350-500 km, i.e. at those distances where both radar systems are able to detect echoes. Importantly, maximum of the 50-MHz velocity is at  $0^\circ$  of the aspect angle (500 km) and coincides well with the position of the maximum in echo power. Velocities of 12-MHz echoes are slightly decreased at distances of 12-MHz echo power maximum (400 km) indicating that the maximum in the 12-MHz velocity does not correspond to the maximum in the 12-MHz echo power. The equatorward shift of 12-MHz echo power is obviously due to additional refraction of these radio waves and the magnitude of the shift agrees well with the model predictions of *Uspensky and Willimas* [1988] and *Uspensky et al.* [1994]. Figure 4 shows the SuperDARN and CRL slant range profiles for the power and Doppler velocity for the westernmost azimuth of 185. Velocities exhibit similar trends with slant range, though the 12-MHz velocity values (circles) are smaller than the 50-MHz velocities (crosses). It is clear also that 50-MHz echoes are shifted to larger ranges at this azimuth.

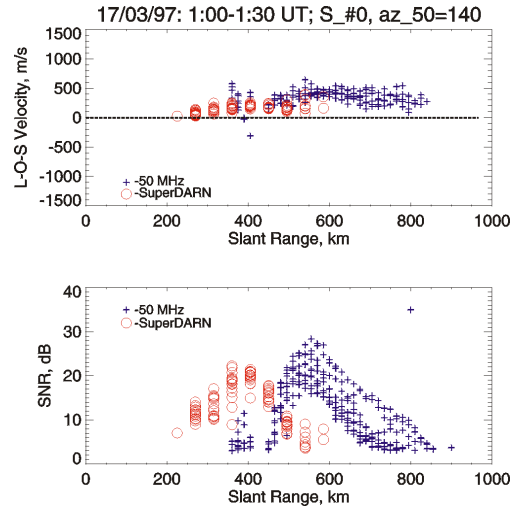


Fig.4

## Discussion

In terms of power we show in this study that echoes are stronger for those areas of the high-latitude ionosphere where the real aspect angles (after ionospheric refraction) are small, thus confirming previous HF measurements. We do not have information about electron density distribution for the event under consideration to make realistic numerical estimates of refraction. However, we do feel that refraction was not strong for the 50-MHz observations since echo power had the maximum at those ranges where geometric zero aspect angles were achieved at 110 km. One needs a low E-region density of less than  $10^5 \text{ cm}^{-3}$  for this to be realistic [*Uspensky and Williams*, 1988, *Uspensky et al.*, 1994]. These “low” electron density are nevertheless significant for refraction of 12-MHz radio waves.

The presented power data allow to estimate the “apparent” aspect sensitivity of 50- and 12-MHz echoes. If one assumes that the maxima of echo power occurs at zero real aspect angles (after refraction), one can estimate that 50-MHz echo power attenuation is of the order of 10 dB/deg (see Figure 2a, 20-dB attenuation over span of  $2^\circ$  in aspect angle at azimuths around 85) while for the 12-MHz echoes (see Figure 2c, 5-dB attenuation over the span of aspect angles of  $2^\circ$ ) it is of the order of 2-3 dB/deg. Such a difference between “apparent” aspect sensitivity of 50-MHz and 12-MHz echoes is in our opinion not so due to the real aspect sensitivity difference of meter and decameter ionospheric irregularities as largely due to significant ionospheric refraction for the 12-MHz echoes that smoothes out a stronger “natural” aspect sensitivity of these irregularities [*Uspensky and Williams*, 1988].

We show that on average, echo power at both 50-MHz and 12-MHz has a clear minimum for directions approximately perpendicular to the magnetic L-shells (assumed direction of the electron flow). As for the direction of the maximum in echo power, there is a difference. The 50-MHz echoes were most

intense for the directions approximately along the magnetic L-shells. One can notice a 20-dB decrease in echo power with the flow angle increase by 90 in Figure 2a. For 12-MHz echoes, even though clearly there is a minimum in echo power for observations perpendicular to the magnetic L-shells, the flow dependence is very weak so that it is difficult to say where the maximum is located. This result in some ways confirms the conclusion of *Hussey et al.* [1999] that the azimuthal distribution of decameter backscatter is different from the meter-scale backscatter. Our observations indicate that close to uniform flow-angle distribution of 12-MHz echoes be sustained not only for low electric fields (when the primary instability is the G-D instability) but also for strong electric fields when the F-B instability can operate in addition to the G-D instability.

In terms of echo Doppler velocity we demonstrate in this study that phase velocities of 12-MHz (12-m) and 50-MHz (3-m) echoes (irregularities) are very comparable at the same slant ranges. The most astonishing result is that these comparable velocities are observed not only for small but for large plasma drifts as well. For strong Doppler velocities (plasma drifts) of more than 500 m/s one would expect that the F-B instability is excited without any doubt and the phase velocity of primary F-B irregularities is saturated at the ion-acoustic speed [e.g., *Kelley and Fejer*, 1980]. The ion-acoustic speed depends on the electric field intensity, ranging from 400 m/s to 600 m/s. In terms of these values, our observations of 600 m/s Doppler velocities at azimuths of 80 are in full agreement with the ion-acoustic saturation ideology (for all scales of linearly-excited F-B waves) if one assumes that we are dealing with enhanced electric fields of more than 50 mV/m. The close velocities of 12-MHz and 50-MHz echoes can be explained by the fact that these echoes are received from different altitudes where the ion-acoustic speed is about the same, the effect known for strong electric field conditions in the auroral ionosphere when the ion-acoustic velocity at altitudes 105-115 km is enhanced due to turbulent heating. Since refraction is significant for 12-MHz echoes, these echoes can come from slightly higher altitudes (say more than 115 km) where zero aspect angle condition can be met easier for the geomagnetic field configuration near Syowa. This explanation is especially exciting if one considers the fact that for observations at azimuth of 80, Figure 3, the 12-MHz velocities are slightly larger (in absolute value) than the 50-MHz velocities.

On the other hand, it is customary to believe (following *Farley and Fejer* [1975]) that ionospheric plasma gradients modify the speed of primary decameter F-B irregularities to smaller values [e.g., *Hanuse et al.*, 1991], see also Figure 5. This effect is progressively increasing with the scale of irregularities so that a decrease of an observed Doppler velocity by more than 2 times can be expected, Figure 5. Our results indicate that this is not the case up to Doppler velocities of 600-700 m/s. Moreover, if one takes into account the fact that 12-MHz echoes might have been received at non-zero aspect angles, one might expect even stronger Doppler velocities of 12-MHz echoes as compared to 50-MHz echoes. We can conclude that the expected effect of gradient-drift contribution to the observed phase velocities of 12-

MHz irregularities [*Farley and Fejer*, 1975; *Hanuse et al.*, 1991] seems as does not exist, at least for the event under consideration.

### Farley-Buneman and Gradient-Drift Instabilities

$$\gamma = \frac{\psi}{1+\psi} [\omega^2 - k^2 c_s^2 + \Omega_e \nu_i \omega / (k L \nu_e)]$$

$$\gamma = 0$$

$$V_{ph} = \omega/k = C_s [(1 + F^2)^{1/2} - F]$$

$$F = \nu_i \Omega_e / (2 \nu_e k^2 L C_s); \quad F \rightarrow 0 \text{ for } L \rightarrow \infty$$

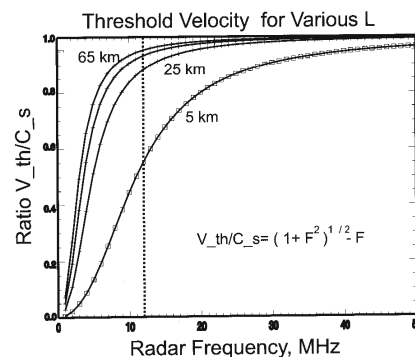


Fig.5

The presented above 12-MHz data show some differences of decameter irregularity characteristics from conventional meter-scale E-region irregularity characteristics. These differences are especially clear for observations along the electrojet. If we look at the histogram of Doppler velocity occurrence for 12-MHz echoes, we see that high-speed echoes are a distinctly different cluster of points contrary to 50-MHz echoes having velocities filling the whole range of velocities 0-700 m/s more homogeneously.

To quantify those differences, an approach of *Milan and Lester* [1999] has been adopted. We made the so called "Watermann plots", i.e., dependencies of spectral width and power versus Doppler velocity and also we plotted a variation of Doppler velocity with azimuth of observations (which is to some extent equivalent to the flow angle of observations). These diagrams are presented in Figure 6. The conclusion from these data is that high-velocity echoes belong to the Class 3 of echoes as introduced by *Milan and Lester* [1999]. Though no serious arguments can be presented at this time, we think that the observed high-speed decameter-scale irregularities are produced by the Farley-Buneman instability and the discovered differences in echo characteristics (Watermann plots) are mainly resulted from various propagation effects that are very significant for HF radio waves.

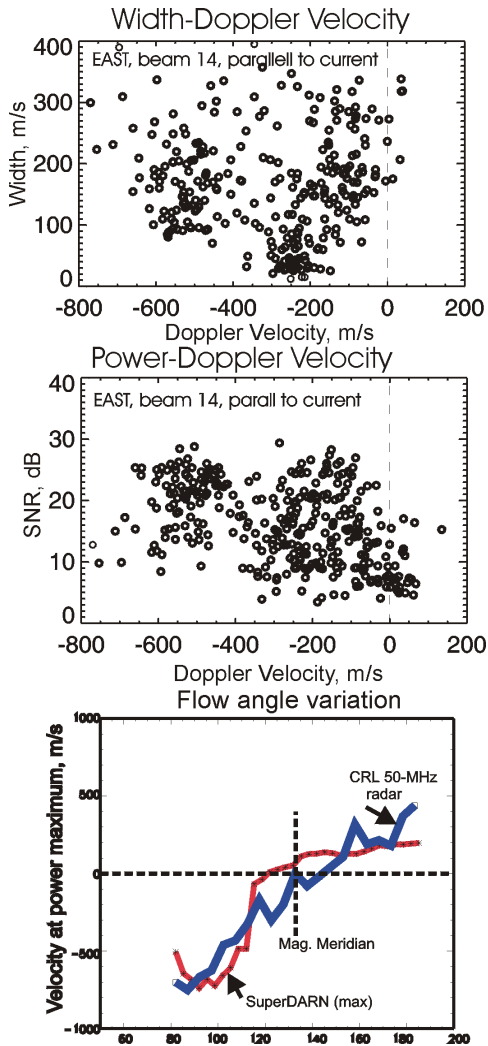


Fig. 6

## Conclusions

In this paper we show that for the short joint interval of 12-MHz and 50-MHz observations:

- Power spatial distribution has an "arc"-like shape with shorter distances for observations perpendicular to the magnetic L shells. The "arc" of echo power distribution follows the zero aspect angle line at both radar frequencies though the 12-MHz signals are consistently shifted by 50-70 km equatorward at all azimuths of observations.
- 50-MHz echoes are much stronger (by about 20 dB) at small azimuths (along the electrojet) while 12-MHz echoes exhibit almost uniform flow angle power distribution with local maxima at some azimuths. At these azimuths, no local enhancements of

12-MHz Doppler velocity is observed. At both radar frequencies, minima of echo power are around magnetic meridian direction.

- Apparent aspect angle effect for the power is of about 10 dB/deg for 50-MHz and 2.5 dB/deg for 12-MHz echoes. Slow power aspect attenuation at 12-MHz is most likely resulted from strong refraction.

- 12-MHz and 50-MHz Doppler velocities are comparable for observations along magnetic L-shells even for large velocity values of up to 500-600 m/s.

- If one assumes that the electric field was distributed uniformly in the radar's F-O-Vs, then the inferred aspect angle attenuation of Doppler velocity for 50-MHz agrees well with measurements of Ogawa *et al.* [1981].

- There is a clear general flow angle variation of Doppler velocity at 50-MHz. For 12-MHz echoes, similar strong variation has been noticed only for eastward radar azimuths. For westward radar directions, the tendency in Doppler velocity flow variation is not clear.

- Presented data indicate that backscatter from the Farley-Buneman waves has different characteristics at meter and decameter scales. Further studies, refining these differences, are required.

## References

- Farley, D. T., and B. G. Fejer, The effect of the gradient-drift term on type I electrojet irregularities, *J. Geophys. Res.*, 80, 3087-3090, 1975.
- Fejer, B. G., and M. C. Kelley, Ionospheric irregularities, *Rev. Geophys.*, 18, 401-454, 1980.
- Hanuse, C., et al., Statistical study of high-latitude E-region Doppler spectra obtained with SHERPAHF radar, *Ann. Geophys.*, 9, 273, 1991.
- Hussey, G. C., C. Haldoupis, A.A. Bourdillon, and D. Andr  Spatial occurrence of decameter midlatitude E region backscatter, *J. Geophys. Res.*, 104, 10,071-10,080, 1999.
- Igarashi, K., K. Ohtaka, M. Kunitake, T. Tanaka, and T. Ogawa, Development of scanning-beam VHF auroral radar system, *Proc. NIPR Symp. Upper Atmos. Phys.*, 8, 65-69, 1995.
- Igarashi, K., K. Ohtaka, M. Kunitake, and T. Kikuchi, Scanning-beam VHF auroral radar at Syowa station, *Proc. NIPR Symp. Upper Atmos. Phys.*, 11, 154-158, 1998.
- Jayachandran P. T., et al., HF detection of slow long-lived E region plasma structures, *J. Geophys. Res.*, 105, 2425-2442, 2000.
- Milan, S., and M. Lester, Spectral and flow angle characteristics of backscatter from decameter irregularities in the auroral electrojet, *Adv. Space Res.*, 23, N10, 1773-1776, 1999.
- Ogawa, T., et al., Aspect angle dependence of irregularity phase velocities in the auroral electrojet, *Geophys. Res. Lett.*, 7, 1081-1084, 1980.
- Sahr, J., and B. G. Fejer, Auroral electrojet plasma irregularity theory and experiment: A critical review of present understanding and future directions, *J. Geophys. Res.*, 101, 26,893-26,909, 1996.
- Uspensky, M. V., and P. J. S. Williams, The amplitude of auroral backscatter: 1. Model estimates of the dependence on electron density, *J. Atmos. Terr. Phys.*, 50, 73-79, 1988.
- Uspensky, M. V., et al., Ionospheric refraction effects in slant range profiles of auroral HF coherent echoes, *Radio Sci.*, 29, 503-517, 1994.
- Villain, J.-P., et al., Obliquely propagating ion acoustic waves in the auroral E region: Further evidence of irregularity production by field-aligned electron streaming, *J. Geophys. Res.*, 95, 7833-7846, 1990.